

Effect of environmental conditions on volcanic plume rise

Hans-F. Graf and Michael Herzog¹

Max Planck Institute for Meteorology, Hamburg, Germany

Josef M. Oberhuber

German Climate Computing Centre, Hamburg, Germany

Christiane Textor

Max Planck Institute for Meteorology, Hamburg, Germany

Abstract. Sensitivity studies were performed with a complex nonhydrostatic volcano plume model that explicitly treats turbulence and microphysics. The impact of environmental conditions such as wind, temperature and humidity profiles was studied for standard observational data. To investigate the wind effects, a two-dimensional Cartesian formulation of the model was used, while for the temperature and humidity effects a cylindrical coordinate system had to be applied, since this treats the entrainment process more realistically. It was found that horizontal wind generally reduces the height of the ash plume. The gaseous part of the plume sometimes may rise higher than without wind owing to the more effective separation between gas and solid material. Besides reduced static stability, the absolute temperature and humidity also increase the plume height. All environmental impacts strongly depend on the strength of entrainment and thus on the quality of the prognostic turbulence.

1. Introduction

Volcanic plumes, consisting of a hot mixture of silicate particles (ash and the larger lapilli), volcanic and environmental gases, and condensed water are one of the most fascinating natural phenomena. The development of the plume is important for the vertical transport of particles and gases. Internal processes such as phase transitions, adhesion of gases to particles, and dissolution into droplets determine the efficiency of the lithospheric source for the atmosphere. Tropopause-penetrating plumes can inject large amounts of sulfurous gases into the stratosphere, where they may persist for years and lead to climatic anomalies. The airborne volcanic ash is hazardous for aviation, and deposited ash can destroy houses and agricultural properties. Heights of eruption columns are still the most important factors to estimate the explosive strength of an eruption. The distribution of proximal and distal fallouts serves as a means to estimate the column height of historic and prehistoric eruptions.

In the 1970s, volcanologists began to study the physics and dynamics of eruption columns with the focus being on sedimentation of ash. *Wilson* [1976] and *Sparks and Wilson* [1976] experimented with one-dimensional top-hat models to study the transport of particles and their sedimentation in eruptive clouds. Microphysical and chemical aspects were not treated in these models. The role of condensational heat of water vapor was considered by *Woods* [1988, 1993] and *Glaze et al.* [1997], only with respect to increased updraft due to latent heat release. Water vapor is one of the most

abundant volcanic gases, and its influence on the plume behavior was discussed in detail based on complex microphysics and diagnostic entrainment by *Herzog et al.* [1999].

The only complex (i.e., including particle dynamics) two-dimensional (2-D) dynamic plume models used for the simulation of volcanic eruptions so far have been those of *Wohletz et al.* [1984] and later of *Valentine and Wohletz* [1989], *Dobran and Neri* [1993], and *Neri and Macedonio* [1996]. These models are conceptually very similar and treat in a relatively small model domain a short-term high resolution in space and time. They predict the time evolution of the flow, momentum, and heat for each constituent and explicitly parameterize the interaction of the components due to exchange of momentum and heat. For this purpose a model concept is needed that resolves timescales of micro seconds. In brief, complete sets of Navier-Stokes equations for each component are solved, which have been only gas and ash in the above mentioned models.

However, a difficulty arises when this model concept is applied to longer timescales, namely, if one is interested not in the explicit resolution of phenomena inside a volcano vent on the scale of a meter, but, as we intend to do, in the link to the large-scale atmospheric flow and chemistry. At larger space and timescales, interactions on the meter scale can be neglected, but many different components have to be treated. The goal to simulate larger spatial scales implies also the need of simulating longer temporal scales. The model concept published by *Valentine and Wohletz* [1989] consumes enormous amounts of computer resources when applied to more than only two components, solved in a bigger domain than of the order of 5 km box size and run over more than 10 min, which is the timescale of dynamic feedbacks due to cloud physics. So their model concept cannot be applied very well with a growing number of components and a coverage of larger spatial and longer temporal scales. This is because each additional component, e.g., water vapor, results in an increase of five more prognostic variables in the three-dimensional case. Therefore a simulation over

¹Now at University of Michigan, Ann Arbor, U.S.A.

Copyright 1999 by the American Geophysical Union.

Paper number 1999JD900498.
0148-0227/99/1999JD900498\$09.00

longer timescales and the need to add a larger number of components to describe the cloud physics immediately result in an impracticable computer code owing to its intense use of memory and CPU time without necessarily bearing higher-quality results because of the immense increase in degrees of freedom and numerical uncertainties.

In order to circumvent that problem, a concept was developed in which each additional component requires only one additional prognostic variable. On the basis of the assumption that particles are small; that is, particles approach their stationary fallout velocity of the order of a second, and not trying to resolve spatial scales down to the meter scale, the explicit description of the components by separate sets of Navier-Stokes equations can be replaced by one set of Navier-Stokes equations for the volume mean of momentum and heat, while the mass of each component is treated by a separate mass continuity equation. The equation of state connects volume mean quantities with the dynamics of single components. This allows one to apply a more elaborate microphysical package or chemistry. After a short introduction of the model concept, we will show results from sensitivity studies for different environmental conditions, such as vertical profiles of horizontal wind, temperature, and humidity.

2. Model Concept

The active tracer high-resolution atmospheric model (ATHAM) was originally designed to simulate explosive volcanic eruptions for a given forcing as a lower boundary condition. In the present version the ATHAM model consists of four modules: The dynamic part solves the Navier-Stokes equation for a gas particle mixture including the transport of active tracers [Oberhuber *et al.*, 1999]. The turbulence closure scheme computes turbulent exchange coefficients for each dynamic quantity [Oberhuber *et al.*, 1999; Herzog, 1998]. The microphysics is based on a Kessler-type parameterization and describes condensation and formation of precipitation. The connected changes in internal energy can have a strong impact on the plume dynamics. All phases of water are included: vapor, liquid, and solid [Herzog *et al.*, 1999]. The soil module computes the amount of deposited particles, ash, as well as water and provides a model-consistent lower boundary condition for temperature and humidity. This means the atmosphere can be heated from the ground, and water can evaporate into the atmosphere from the soil. A physicochemical module treats the interaction of gases and condensed matter in the plume [Textor, 1999]. The model is written in a modular structure. It is easy to couple to it modules of different levels of sophistication for special processes. The coupling is organized via defined interfaces.

ATHAM is fully three dimensionally formulated with an implicit time step scheme. The flux form of the transport equations is employed for all tracers. For sensitivity studies and to test the model, two different types of 2-D versions are implemented: One Cartesian 2-D version computes on a vertical slice of the 3-D model and allows for the study of cross-wind effects. The 3-D counterpart is a fissure eruption with infinite length. The second 2-D version represents cylindrical coordinates. No cross-wind effects can be studied, but the dilution of the mixture corresponds to the 3-D case in an atmosphere at rest. A 2-D Cartesian version underestimates entrainment owing to the missing third-space direction. This is better treated by 2-D cylinder coordinates, where the full surface of the plume is available for entrainment.

Two-dimensional (3-D) simulations are performed on a stretched grid with $127 \times 127 \times 4$ (127) grid points. The horizontal domain is typically 250 km; the vertical is 50 km. In the center of

the model area we use a spatial resolution of 100 m or, in some special cases, 50 or even 20 m. At the fringes of the model domain the horizontal resolution is of the order of several kilometers. The simulation time is typically 1 hour with time steps being dynamically adjusted to the Courant-Friedrichs-Lewy (CFL) criterion. Time steps are normally smaller than 1 s during the active eruption phase.

2.1. Dynamical and Thermal Equilibrium

The special feature of ATHAM is its ability to treat active tracers. In contrast to passive tracers normally used in atmospheric models, active tracers can occur in any concentration, affect the equation of state, and can therefore have a strong influence on the dynamics of the system. In case of a volcanic eruption, the mass fraction of silicate particles close to the vent is often higher than 90%. Active tracers such as silicate particles influence the dynamics of the system in two ways: First, in the presence of solid or liquid particles the density of the mixture is, in general, greater compared to the density of the gas phase alone. As a consequence the buoyancy force can be strongly reduced. Second, silicate particles can act as a source of heat and thereby change the temperature distribution and the dynamics of the system toward increased buoyancy.

Without additional assumptions the description of a multicomponent system of active tracers requires one set of dynamic and thermodynamic equations for each component with interactions between them (Figure 1, left). This requires enormous computer resources for a large number of active tracers. Wohletz *et al.* [1984] and Neri and Macedonio [1996] therefore use only one or two par-

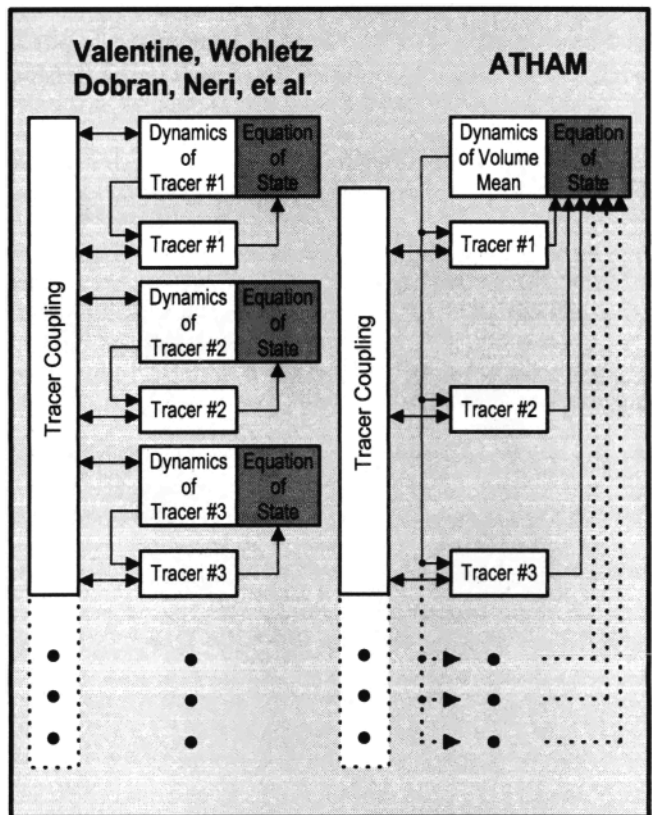


Figure 1. Schematic of the new approach of the active tracer high-resolution atmospheric model (ATHAM) as compared to previous complex volcanic plume models [Valentine and Wohletz, 1989; Dobran and Neri, 1993]. See text for description

ticle classes. Our goal is to describe the plume during its whole lifetime, including the thermodynamics and microphysics of water and a large number of other chemical species. Therefore we need another level of abstraction that allows the parameterization of the total effect of the active tracers without treating each component with a separate set of prognostic equations (Figure 1, right).

The main assumption of ATHAM is only a minor restriction in the case of a plinian eruption plume: All particles are small. This has two consequences in physical terms: First, the system is at all times in dynamic equilibrium. That means we assume an instantaneous momentum exchange between particles and gas. All particles move with their terminal velocity relative to the mixture, which simplifies the description of sedimentation. The assumption of dynamic equilibrium is, for the given resolution of ATHAM and typical densities and accelerations, valid for ash (particles smaller than 2 mm) and also for lapilli (particles of 2–64 mm) consisting of rough and gas rich material as long as their terminal velocity remains small. If the terminal velocity of the particles is larger than ~10 m/s, their deviation from the concept of dynamical equilibrium is no longer negligible within the frame of our problem of simulating strong volcanic eruption plumes [Oberhuber et al., 1999].

The second assumption requires that the system is at all times in thermal equilibrium. Tracers can act as a source of heat, but the temperature exchange is instantaneous. Thermal equilibrium can be accepted only for particles of diameters not larger than 1 mm that have adjustment times smaller than 1 s. These include practically all ash. For larger particles a prognostic temperature equation would be necessary, which, if needed, is easily included in the model.

The assumption of small particles strongly reduces the number of prognostic quantities and allows for the treatment of a multi-component system with many active tracers. The dynamic behavior of the gas particle mixture is described by five prognostic equations for the three momentum components, pressure, and temperature. For each tracer one additional transport equation has to be solved. Apart from two types of silicate particles (ash and lapilli), five types of tracers for the microphysics of the system are implemented in the present version: water vapor, cloud water, precipitable water, ice, and graupel. Additional tracers can be included. Active tracers and dynamic variables are coupled because of bulk density and heat capacity of the mixture.

2.2. Turbulence

Generally, the plume of a plinian eruption is described as a jet regime close to the vent and a convective regime above. The jet regime is characterized by the consumption of initial momentum and laminar character of the flow. The convective regime is dominated by buoyancy forces. Initially, the bulk density of the erupted hot gas particle mixture is higher than the density of the surrounding atmosphere. Without entrainment, followed by sedimentation of heavier material and separation between the gas and solid and liquid phases, no plume could develop. The amount of entrainment determines the largescale behavior of the plume. Microphysical processes are dominated by entrained water vapor. Except in very dry environments, the water vapor released by the volcano is of secondary importance. Hence the correct treatment of entrainment, which is a function of turbulence, is essential.

In atmospheric problems one usually assumes an equilibrium of turbulent quantities and a local isotropy of turbulence. Turbulent exchange is locally the same in all directions. This is not valid for an eruption plume: The timescales of the physical problem are smaller or in the same range as the timescales of turbulence. The

conditions under which turbulence develops change faster than the turbulent quantities can adapt. This requires that the history of the development of turbulent quantities must be taken into account. Transport processes and the existence of a mean density gradient cannot be neglected. The dominant influence of buoyancy leads to an asymmetry between horizontal and vertical components of turbulent quantities.

Following the formulations of Kolmogorov-Prandtl, the turbulent exchange coefficient for momentum is given by a turbulent length scale and the turbulent kinetic energy. This formulation [Oberhuber et al., 1999; Herzog, 1998] is based on the idea that turbulent processes are illustrated through eddies of different size. The turbulent energy is a measure of the intensity of turbulent eddies, the turbulent length scale for the average size of turbulent eddies, and the exchange coefficient for the efficiency of turbulent eddies.

To take into account the anisotropy of horizontal and vertical components, the original formulation of Kolmogorov-Prandtl is extended under the assumption that the anisotropy of the exchange coefficients is only expressed in the anisotropy of the turbulent energy. The turbulent length scale is assumed to be isotropic. The chosen formulation guarantees the original formulation in the isotropic case. The horizontal and vertical components of the turbulent kinetic energy as well as the turbulent length scale are simulated by a set of three coupled prognostic equations and solved numerically.

To describe buoyancy effects in turbulent processes, we have to use the potential density: This is the density of a gas particle mixture if it is brought to a reference pressure. In the case of no active tracers this leads to a formulation, which is equivalent to the standard formulation with the potential temperature. There are two types of compressibility effects: density and Mach number effects. In the present version of the turbulence scheme we have added a simple correction term for the Mach number effects. Particle gas interaction as well as particle-particle interaction are neglected at the moment.

2.3. Coordinate Systems

Performing simulations on a vertical slice of the 3-D model, the behavior of typical volcanic eruptions can be simulated reasonably [Oberhuber et al., 1999; Herzog et al., 1999; Textor, 1999]. At the beginning of the simulation the model is initialized with horizontally homogeneous profiles for temperature, relative humidity, and wind with the assumption of a hydrostatic initial state. The flow over a 3000 m high volcano leads to the development of turbulence, mostly concentrated at the top of the volcano. It shows the formation of a boundary layer, an orographic cloud, and a lee wave (Figure 2).

The use of cylindrical coordinates allows for the investigation of the first period of a volcanic eruption under realistic boundary conditions, not only for the temperature and exit velocity but also for the composition of the erupted material and the mass eruption rate. The entrainment and mixing of the plume with ambient air is treated better in cylindrical coordinates than in 2-D Cartesian coordinates, which underestimate entrainment due to the missing third dimension.

Results from simulations with finer grid resolution can be used to estimate a forcing for a coarser model grid. This simple nesting technique combines processes of smaller scales close to the vent and the large-scale behavior of the plume.

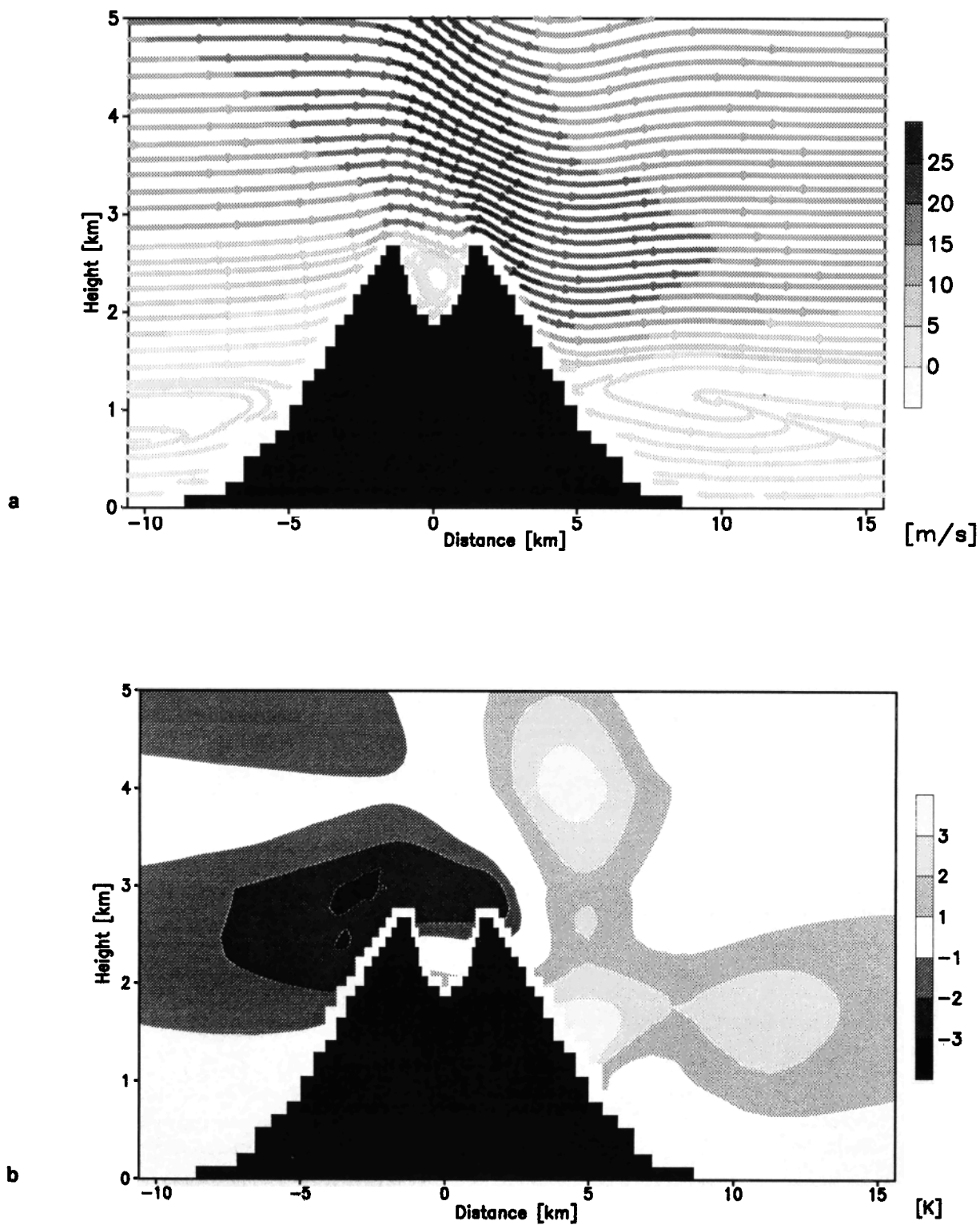


Figure 2. Quasi-stationary solution of ATHAM for (a) wind, (b) temperature anomaly compared with initial atmosphere at rest, (c) condensed water, and (d) turbulent exchange for the boundary conditions from Figure 3 after 15 minutes spin-up.

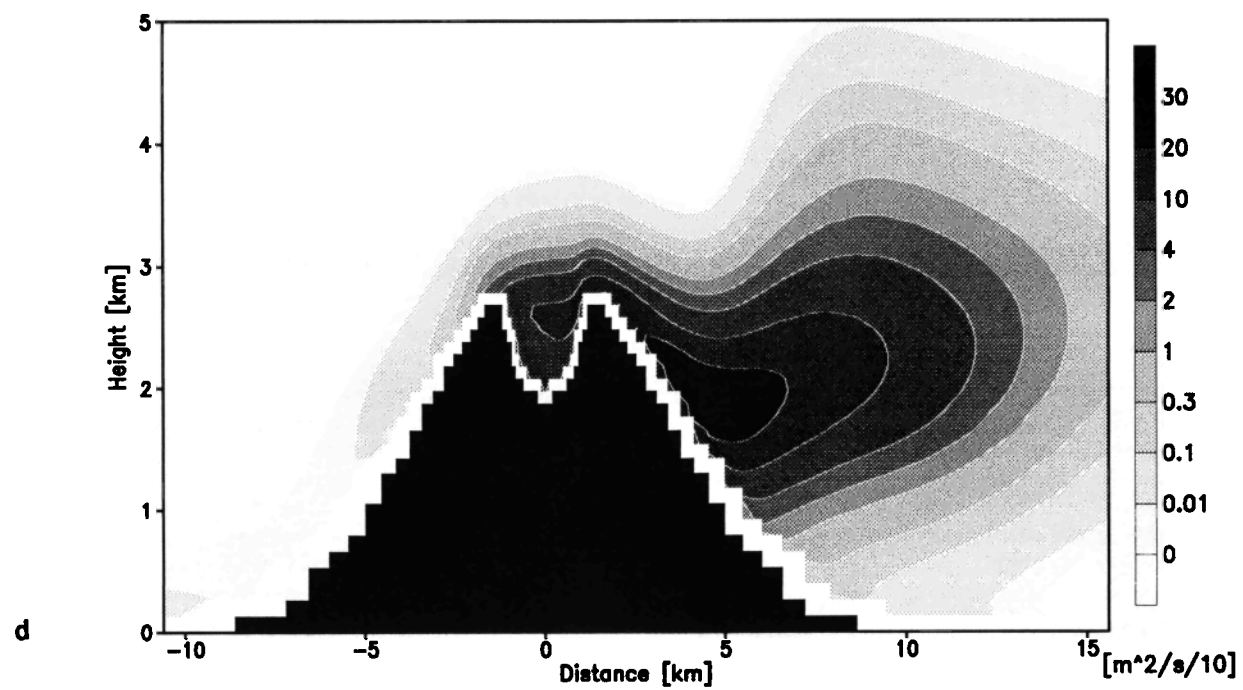
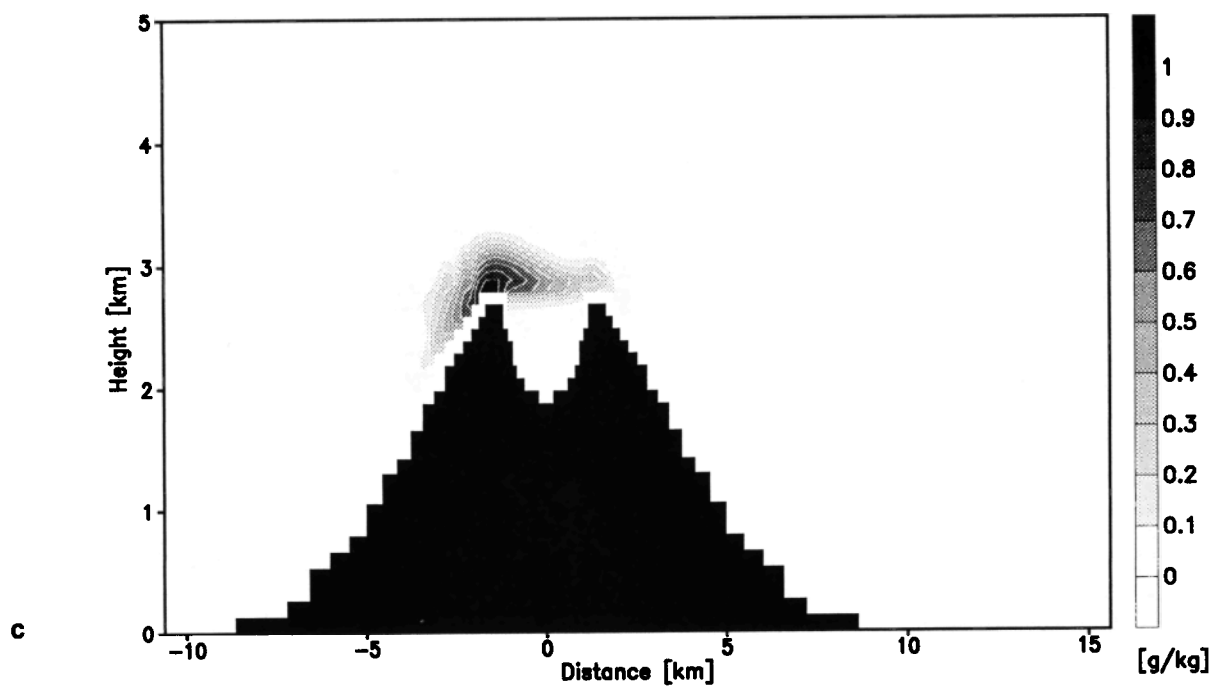


Figure 2. (continued)

2.4. Plume Chemistry

The composition of plinian-type volcanic particles is highly variable for different volcanoes. By far, the highest fraction of tephra is built of aluminosilicate glass shards formed by gas bubble bursting through liquid magma. Besides, silicon and aluminium particles contain different amounts of oxides, halides, and sulfates of Na, K, Mg, Ca, Fe, Zn, and Cu and a variety of trace elements [Hobbs *et al.*, 1982; Smith *et al.*, 1982; Rose *et al.*, 1982; Varekamp *et al.*, 1986]. Salt crystals independent of ash as well as salt coated ash particles, sometimes in acid aqueous solution, have been observed at different locations [Smith *et al.*, 1982; Chuan, 1994] during in-situ aerial sampling of volcanic plumes.

A plume chemistry model has been developed to treat the relevant heavy metal reactions and the chemistry of oxygen, hydrogen, nitrogen, sulfur, chlorine, and methane species in the gaseous as well as the liquid phase. A special emphasis is put on the chemistry of chlorine and sulfur species, which are the most important gases in volcanic emissions with respect to climatic relevance [Textor, 1999]. CO₂, although the most abundant volcanic gas, is not important for atmosphere chemistry in the timescales considered here. The total lithospheric contribution to atmospheric CO₂ is by a factor of 100 smaller than anthropogenic sources [Schmincke, 1993].

2.5. Constraints and Advantages

The constraints and advantages of our model concept can be summarized as follows. A constraint for ATHAM is that our model concept assumes an instantaneous exchange of momentum and heat between the components of the mixture of gas, liquid, and solid particles. Thus a time resolution of less than a few seconds is a limit for applications of ATHAM. An advantage of ATHAM is that the computer code is cheap in memory and CPU time. This is due to the use of only one set of Navier-Stokes equations for the volume mean momentum and heat content and the use of efficient solution techniques for the implicit time-stepping scheme. Additional modules, already realized are cloud physics, turbulence closure, soil, and chemistry, are easy to add. Additional tracers cost only the memory and CPU time for one prognostic equation. Because of the memory-saving programming (currently the 127 × 127 grid size version requires only 6 Mwords of memory), there is enough potential to add a large number of additional tracers that are allowed to feedback dynamically owing to their high mass concentration. The model domain can be extended to scales appropriate for the plume development in the first hours, even of larger eruptions.

Within the constraint to solve only one set of Navier-Stokes equations the additional assumption to predict only the volume mean heat content can be removed easily. If particles are allowed to be bigger, the thermal equilibrium between particles and gas is no more valid within timescales of seconds. By adding further prognostic equations for bigger particles such as lapilli and a prognostic treatment of the heat exchange, at least the assumption of thermal equilibrium can be removed without losing the efficiency of ATHAM.

Our model domain has normally 250 km horizontal and 50 km vertical resolution and typically predicts 1 hour. The earlier models cover a model domain of 10 km horizontally and 5 km vertically. This limits the simulation time to a few minutes, since then border effects dominate the solution. Because we integrate over longer timescales, water vapor and all processes to gain latent heat, i.e., microphysical processes, are needed. The same argument applies for turbulence as its length scale, and thus its efficiency to mix properties within scales resolved by the model grid grows in time and thus

becomes nonnegligible. In addition, we can apply a mean background state, i.e., geostrophic flow, and temperature and humidity profiles, which allows us to study the link between the large-scale weather and the volcanic plume.

3. Background Experiment

The ATHAM model is a complete nonhydrostatic limited area circulation model. Therefore a first test of its performance will be an orographic overflow simulation. The model is used in 2-D Cartesian coordinates over a horizontal domain of 250 km and 50 km in the vertical. The horizontal and vertical resolutions of the model grid are different with the highest resolution of 100 m just above the mountain peak and about 5 km at the model boundaries. The vertical and horizontal resolution can be seen from the step-like contour of the model mountain (shown as black in all figures). This is the standard configuration. In the center of the model area a mountain ridge exists with a height of 3000 m above the surrounding flatlands. The peak has a 2 km wide depression of 700 m (a caldera). Background vertical pressure, temperature, humidity (mean tropical conditions [McClatchey *et al.*, 1972] in the standard case), and typical wind profiles derived from the European Centre for Medium-Range Weather Forecasts (ECMWF) reanalysis data are prescribed at the edges of the model domain. The wind blows from the left. The initial state of the atmosphere is found by letting the model run with these boundary conditions without any volcanic forcing until a quasi-stationary circulation is reached (Figure 2). All the typical features of orographic flow can be found. There is enhanced flow above the mountain, and a lee wave develops to the right of the obstacle. Cooling occurs on the windward side, leading to condensation of atmospheric water vapor and the formation of a mountain cloud. Leeward, typical warming by sinking of dry air leads to larger temperature anomalies than at the upstream side of the mountain. Turbulent energy is increased in the peak region and especially at the leeward peak. Having seen that the model is able to describe basic features of observed atmospheric behavior in a simplified terrain and also in other similarly simple experiments in addition to several sensitivity studies [Oberhuber *et al.*, 1999; Herzog *et al.*, 1999; Textor, 1999], we believe in the model's ability to also simulate volcanic plumes at least qualitatively correctly.

4. Impact of the Environment on Volcanic Plume Rise

Before our studies, volcanic plume simulations were always performed in an environmental atmosphere that was specified quite simply using standard atmospheric profiles. The influence of horizontal wind shear was not studied systematically, since this is impossible in radial symmetric models. Here we want to study such effects in more detail.

4.1. Wind Effects

For the estimation of the effect of horizontal wind on the plume behavior, we again use Cartesian coordinates in a geometry like in the standard background experiment described before. We performed four simulations of a standard volcanic eruption in an atmosphere at rest, with a mean wind profile and modifications of the wind, once the wind was increased in the lower troposphere and another when the wind was reduced in the middle and upper troposphere. The profiles are tropical ones with the tropopause at 17 km. The relative humidity has a second maximum just below the tropopause because of temperature effects (Figure 3). The standard vol-

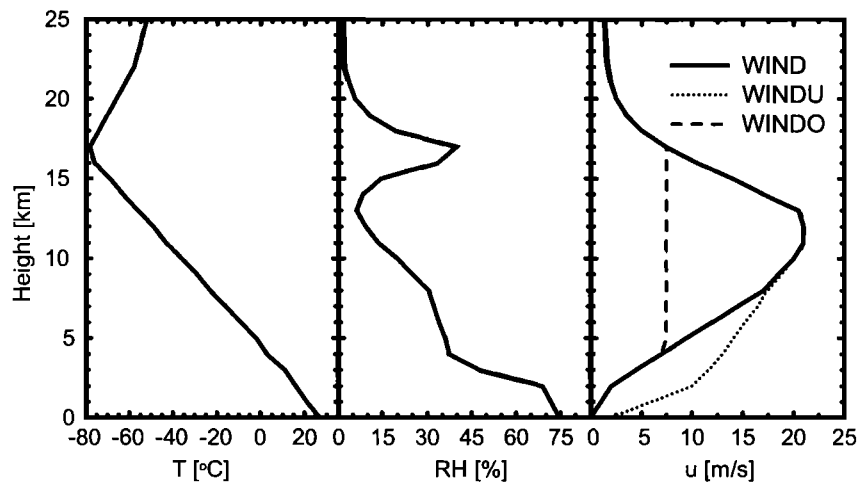


Figure 3. Meteorological boundary conditions for the reference experiment. The vertical profiles of temperature (T) and relative humidity (RH) correspond to tropical conditions [McClatchey *et al.*, 1972]; the standard wind profile (u , WIND solid line) is taken from European Centre for Medium-Range Weather Forecasts (ECMWF) reanalysis data [Gibson *et al.*, 1997]. The other wind profiles are for strengthened lower tropospheric (WINDU) and reduced wind (WINDO), respectively. The wind blows from the left.

canic eruption parameters (Table 1) had to be scaled to the resolution of the model as described by Herzog [1998].

The study of horizontal wind effects on the development of the plume in 2-D Cartesian coordinates will overestimate the effect to a certain degree because of the unlimited extension of the mountain ridge in the third dimension. This leads to stronger acceleration of the wind over the obstacle and thus to a stronger bend-over of the plume than is to be expected for a single mountain in a 3-D model. This means that the dynamical effects are stronger in the model than in nature. On the other hand, thermodynamic effects based on the microphysical transformations will be underestimated because of the neglect of entrainment from the third direction. However, the wind-induced differences, mainly for ash and water vertical distribution, are dramatic and will have to be considered even when they are somewhat reduced. Figure 4 shows the horizontally integrated vertical distributions of ash, lapilli, and total water for the four experiments with idealized atmospheric profiles from Figure 3 for a time of 25 min after the beginning of the eruption. Very clearly, the introduction of horizontal wind leads to a strong reduction of the height of the ash and water plume, which for the standard wind is 4000 m lower than in an initially resting atmosphere. Important also is that the maximum of the ash load is at 15 km in the no-wind case but at 9 km in the standard wind case. The stratospheric injection of ash is reduced from 30% in the no-wind case to 3% of the total emitted ash in the standard wind case. The effects on the vertical ash distribution between different wind profiles are not as important. Generally, a weaker wind leads to higher plume rise.

In the case of the vertical distribution of lapilli, which has a significantly higher fall velocity than ash particles, the shape of the vertical wind profile is very important. While the maximum load of lapilli in all cases is at 3000 m above surface (after 25 min a significant amount of all ejected lapilli has been transported to altitudes well below the peak of the volcano), in the case of intensified lower tropospheric winds from this height the lapilli concentration decreases sharply, while for the other wind profiles, only minor differences exist up to the upper troposphere. Again, in the windless case, lapilli can reach the highest altitudes. In Figure 5 the reason for these differences is shown as an example of the distribution

of ash in a subdomain of our computing area 25 min after the beginning of the eruption. The increased wind in the lower troposphere leads to a strong bend-over of the plume, which, owing to contact with the rim of the caldera, loses kinetic energy. This strengthens the bend-over and leads to an increased deposition of particles and a decrease of the plume density. While in the standard wind experiment, 25 min after the beginning of the eruption, not more than 10% of all lapilli are deposited at the ground, in the case of stronger lower tropospheric winds, 65% has already reached the ground. The bend-over of the plume reduces the residence time of lapilli in the strong updraft region and thus enhances its effective sedimentation velocity. The effect on ash is less strong, since its terminal velocity is much smaller. In the strong wind system, only 5% of all ash reached the ground after 25 min compared with practically no deposition in all other cases.

The consideration of horizontal wind increases the rate of entrainment of ambient air by increased turbulence. Ten percent more

Table 1. Volcanic Forcing

Parameter	Value
Vent diameter, m	60
Exit velocity, m/s	250
Temperature at the vent, K	1200
Gas fraction, weight%	3
Water vapor fraction of total gas, weight%	67
Bulk density at the vent, kg/m ³	5.52
Mass eruption rate, 10 ⁶ kg/s	3.90
Particle size, μm	2
	50

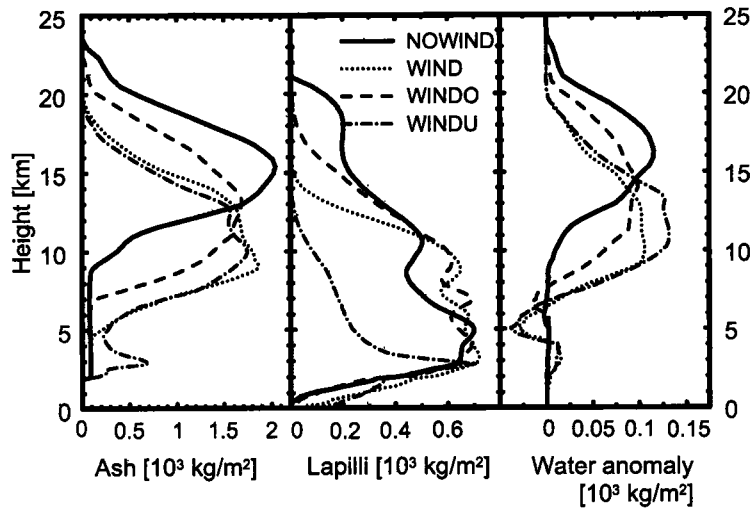


Figure 4. Vertical distribution of ash, lapilli, and water for the experiments with different horizontal wind at 25 min after the start of the eruption. Water anomaly denotes the difference of water at a certain level in the simulation versus the undisturbed initial state.

water vapor is entrained into the plume in the standard wind case compared with the atmosphere initially at rest. Nevertheless, the amount of released latent heat is reduced by about one third because of the lower plume with higher temperatures, leading to reduced condensation in the case with horizontal wind. Generally, wind leads to a lower altitude of the condensation height and less transport of water into the stratosphere. A strengthened wind in the lower troposphere, leading to bend-over at the caldera rim, can overcompensate the negative effect of decreased condensation by enhanced entrainment in the humid lower layers of the troposphere. In our strong wind simulation we found 60% more latent heat production than in the standard wind regime.

Even though the plume loses energy by increased turbulence and friction when wind is considered, this does not affect the transport of gases in the same direction. The deceleration of the vertical velocity component due to the bend-over in low altitudes leads to a more rapid separation of hot rising gases and heavy sedimenting solid particles. Even when the horizontal winds induced by a violent eruption are stronger than those in the preeruptive atmosphere, the background winds lead to distinct changes of the horizontal distribution of ash (Figure 6), in addition to the above mentioned influence on the vertical distributions.

In contrast to earlier simulations with simpler models [Carey and Sparks, 1986], there is only a minor upwind transport of ash.

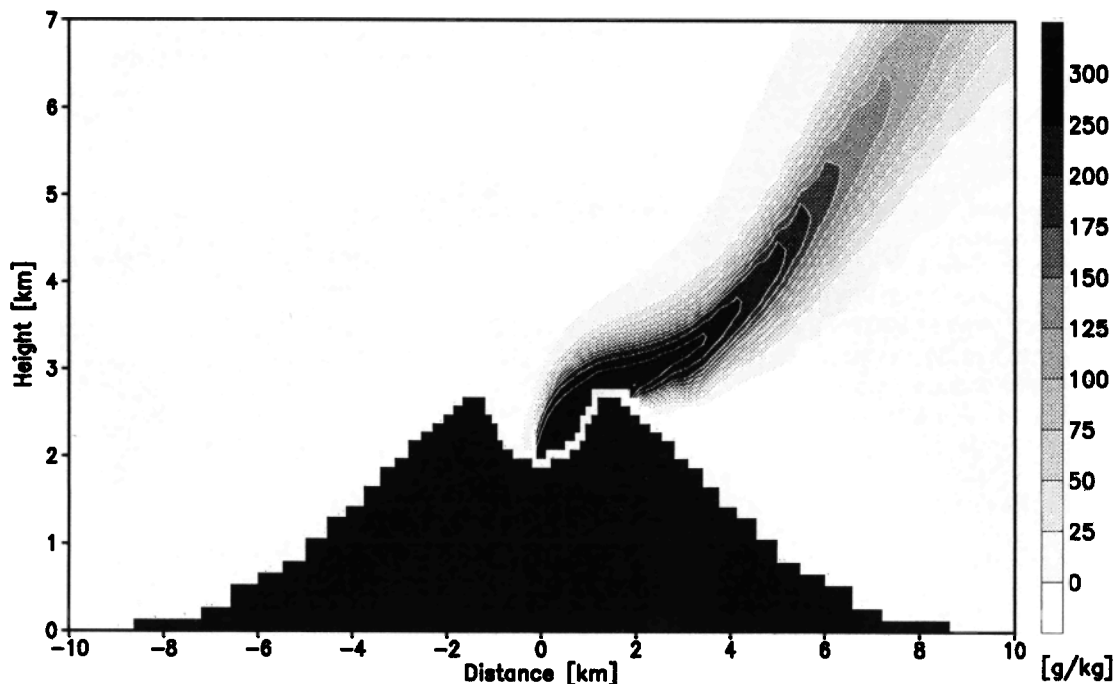


Figure 5. Specific concentration of ash particles in the WINDU experiment at 25 min after the beginning of the eruption.

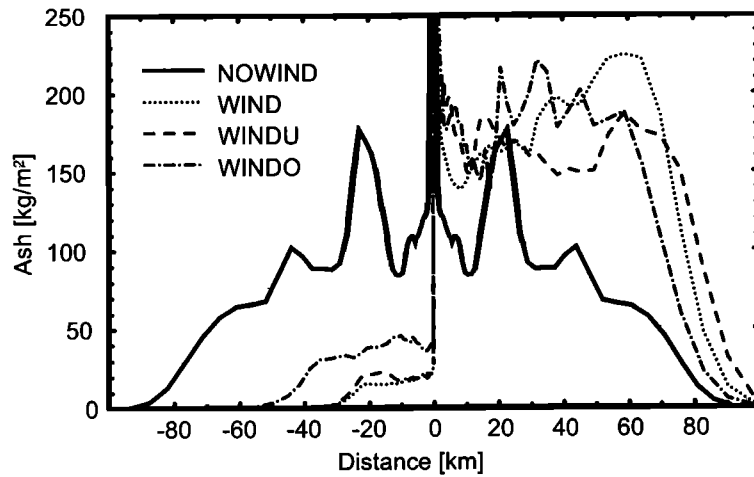


Figure 6. Horizontal distribution of the vertically integrated mass of ash for different wind regimes 25 min after the start of the eruption.

The ash distribution is highly asymmetric, the area of significant ash loading is reduced drastically, and the gradient of the vertically integrated load at the downwind and the upwind edges of the ash plume is much sharper than in the case of missing background wind and is also sharper than in earlier simulations [Carey and Sparks, 1986]. Many of these differences are determined by the circumstances in the umbrella region, where in our simulation the maximum wind from the left blows between 9 and 14 km (Figure 3), just at the height of the biggest ash concentration, i.e., in the umbrella region (Figure 4). In the no-wind case the umbrella region is higher and the maximum horizontal wind influences only the lower part of the umbrella region. Thus it is not only the superposition of wind, plume dynamics, and fall speed that determines the deposition of volcanic ash but also the interaction of all these quantities during the whole process of plume development. The updrafts and downdrafts produced by the buoyant plume lead to strong inhomogeneities such as the maxima ~ 20 km upwind and downwind from the vent seen in Figure 6. Earlier simulations used idealized winds that were smooth enough to produce gauss-type distribution of the isopleths [Carey and Sparks, 1986].

4.2. Environmental Temperature and Humidity

The fact that thermal stability, as measured, e.g., by the vertical temperature gradient, must have an impact on a buoyant volcanic plume is obvious and was shown long ago with simple models [Woods, 1988; Glaze et al., 1997]. However, there is another effect apart from the vertical temperature gradient which may be important. That is the initial entrainment of ambient air and moisture, which leads to a decrease in density and, after condensation of water vapor, to the release of latent heat and further vertical acceleration. The entrainment rate is dependent on the evolving turbulent energy, which in older models has been chosen arbitrarily and constant in a way that the final result of the model (i.e., maximum plume height or sedimentation fan) is in accordance with observations. However, the conditions that are supposed to exist during the plume development are not always very realistic. While the importance of a realistic treatment of turbulent processes and microphysical processes for the plume energetics has been discussed previously by Herzog et al. [1999], here we focus on the effect of environmental conditions. These conditions influence plume development primarily via entrainment.

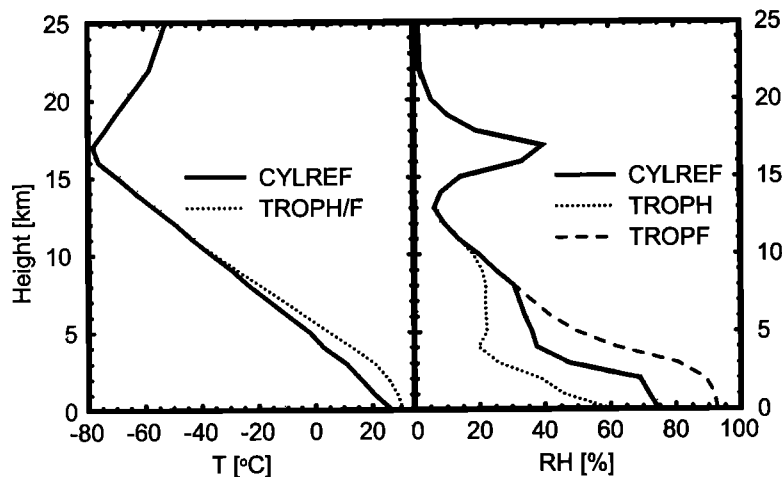


Figure 7. Meteorological conditions (temperature (T) and relative humidity (RH)) for a tropical eruption. Besides the standard experiment (CYLREF, solid line) a warmer (TROPH) and a warm/moist (TROPF) case are also shown.

In order to treat the process quantitatively as appropriately as possible, we have to apply cylindrical coordinates. This means that we cannot account for any effects of a vertically changing wind field. This may lead to an underestimation of the entrainment as discussed above. Besides the change in the coordinate system, the model geometry remains. Our reference experiment is, with the exception of neglecting horizontal wind, the same as the one discussed in section 4.1. It is a tropical atmosphere corresponding to *McClatchey et al.* [1972]. In addition to this, we used data from the same authors to describe typical midlatitude vertical profiles for summer and winter (Figures 7 and 8). The main difference between the experiments lies in the tropopause height, which is at 17 km in the tropics and at 13 (10) km in the midlatitude summer (winter). In winter, in addition, the temperature at the surface and up to the tropopause is reduced of the order of 20 K. The maximum in relative humidity that occurs in the tropics at the tropopause is much smaller in midlatitudes. For the tropics two more experiments were performed such that the temperature profile was changed toward a 10 K higher temperature at the elevation of the crater of the volcano. This may, for example, be an effect of the daily cycle of temperature. A stable vertical temperature gradient was assumed. Above 11 km height there is no difference between the temperature profiles of the two tropical cases. The relative humidity was determined under the assumption of identical specific humidity. This is a reasonable assumption for air mass internal diurnal changes. In a third tropical experiment (humid tropics) the same temperature profile was used as in the warm tropical case, but the specific humidity was changed to a value about twice that in the warm tropical case. The characteristics of the volcanic eruption are described in Table 1. Thus we now have one reference (CYLREF), one tropical warm (TROPW), and one tropical warm and humid (TROPF) experiment, as well as one midlatitude summer (MIDSUM) and one midlatitude winter (MIDWIN) experiment. The results of the respective simulations are given in Figures 9 and 10 for a time of 25 min after the beginning of the eruption. The vertical distributions of horizontally integrated ash concentration and water exceeding the ambient concentration (water anomaly) for the midlatitude simulations (Figure 9) show that the mean meteorological condition significantly influences the plume behavior. Under midlatitude summer (MIDSUM) conditions the ash plume rises 1000 m less than in the tropics. It is stopped at the tropopause at 13 km height. Only a small amount of cloud ice and water vapor (~1% of the total plume water) reaches the stratosphere. Cloud ice consists of small

needles or plates of frozen water that are templated in the air. This value will be typical also for other gases that are not dissolved in the condensed water or adhere at the ash, such as SO_2 . Even more clear is this effect under midlatitude winter conditions. The total plume height is reduced by another 1000 m; but because of the lower tropopause height (10 km) nearly one third of the erupted ash particles reaches the lower stratosphere and, of the plume water, even > 50% enters the stratosphere. Most of it (90%) is in the form of ice crystals; the remainder is as gas.

As shown for the tropics, the actual weather conditions also play an important role for plume development. The results of the TROPW and TROPF experiments are given in Figure 10. In comparison to the standard experiment CYLREF, warming and moistening of the lower troposphere both lead to increased height of the ash and water plumes. Even the higher temperature alone, which may develop in the course of a day, leads to 2300 m higher plumes. The water plume already reaches the tropopause at 17 km. The ash plume stops ~ 500 m below. After 25 min, water vapor entrainment is in TROPW ~ 10% above the reference value and 90% of the water is condensed, while in CYLREF it is only 75%. Hence the effect of latent heat release is enhanced.

The vertical temperature profile has a larger effect on the final plume height than the slightly enhanced microphysical processes. Simulations with and without microphysics revealed that owing to phase changes of water, the total thermal energy is increased 13% in CYLREF and 17% in TROPW, resulting in a difference in plume height due to the microphysical effects of only 300 m.

The doubling of the water vapor content in the lower troposphere (TROPF) results in a strongly enhanced influence of the microphysics on plume behavior. Compared with only higher temperature effects of TROPW, the increased humidity leads to a 2200 m higher plume. Changed atmospheric conditions alone increase the plume height in TROPF by 4500 m (30% more than the height in the reference experiment). This is enough to rise into the stratosphere. The plume spreads below the tropopause level, and therefore only 10% of the total ash and 14% of total water (99% as ice crystals) are found in the stratosphere 25 min after the beginning of the eruption. The amount of entrained water vapor is nearly 1 order of magnitude larger than in the reference experiment. Hence microphysics become more important. They contribute 4000 m (in CYLREF only 1500 m; in TROPW, 1800 m) to the total plume height, as computed with simulations excluding microphysics.

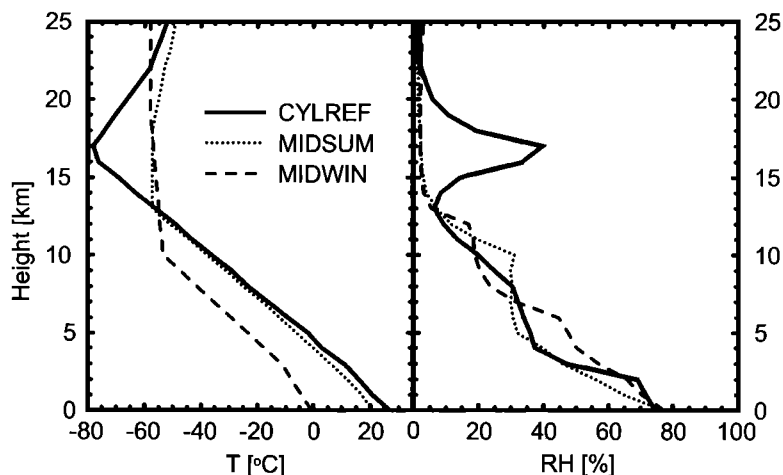


Figure 8. Same as Figure 7, but for midlatitude midwinter (MIDWIN) and midsummer (MIDSUM).

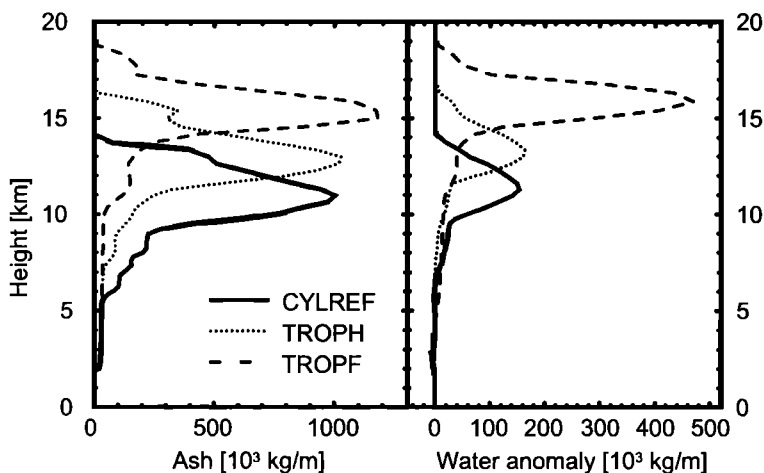


Figure 9. Vertical distribution of (left) ash and (right) water anomaly per 1 m vertical column for the different mid-latitude experiments as defined by the T and RH profiles in Figure 7, 25 min after the beginning of the eruption.

5. Conclusions and Discussion

Applying a new complex, nonhydrostatic model to a standard violent volcanic eruption, we performed a series of sensitivity studies to investigate the influence of environmental conditions on the plume development. In our discussion we concentrate on ash and water plumes, which most clearly indicate the strong impact of the environment even in the case of a strong volcanic eruption.

For reasons of computing efficiency we applied two two-dimensional versions of ATHAM instead of the full three-dimensional original. The Cartesian version is capable of treating crosswind effects but, owing to the missing third dimension, underestimates entrainment. The axisymmetric version is exact for entrainment in an atmosphere at rest but cannot handle crosswind effects. Neither of the two versions can treat the bifurcation of volcanic plumes that was discussed by *Ernst et al.* [1994] for strongly bend-over plumes. However, here we deal with an eruption easily reaching the tropopause level, where the latter effect is negligible anyway [*Ernst et al.*, 1994]

Generally, we found that the horizontal wind field can dramatically change the shape and height of the volcanic plume. The stronger the wind is, the lower the top of the plume will be.

Under special circumstances, the bend-over of the plume may induce early separation of gas and particles, thereby leading to a higher gas plume and more gas being injected into the stratosphere. Thus the climatic consequences of a volcanic eruption, which are determined mainly by the amount of sulfurous gases (SO_2 , H_2S) injected into the stratosphere, are strongly dependent on the environmental conditions during the time of the eruption.

The standard treatment of deposition of volcanic ash as based on *Sparks and Wilson* [1976] and *Carey and Sparks* [1986] including crosswinds and recently discussed by *Woods and Bursik* [1991] supposes that all ash is transported to the umbrella of the volcanic plume or “support envelope” [*Carey and Sparks*, 1986], where their terminal fall velocity equals the idealized upward velocity in the plume, which then is shifted by the horizontal wind, and the deposition can be calculated by vector addition of the vertical wind profile and the sedimentation velocity of the solid particles. The vertical transport of ash is normally computed by simple top-hat or axisymmetric models which, during the plume development, do not allow one to consider horizontal wind. As our simulations show, this leads to an overestimation of the height of the ash and lapilli plume; and, in addition, it leads to an overestimation of the horizontal extension of the ash plume. Further, if the wind drift of

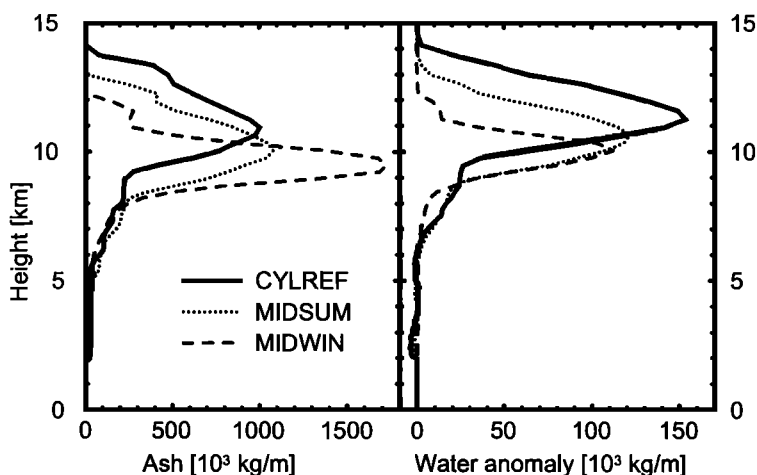


Figure 10. Same as Figure 9, but for T and RH taken from Figure 8.

the whole plume is not accounted for, the distribution of the total load of ash is overestimated to the windward side and underestimated to the leeward side of the source. This may lead to misinterpretations of the sediment fan in terms of plume height and volcanic and environmental conditions for events for which direct observations of these parameters are not available. Important horizontal inhomogeneities of the ashfall can only be explained by the superposition of plume-induced and ambient wind fields.

Not only the wind but also the temperature and humidity stratification are important factors for the volcanic plume evolution. If only vertical stability of the atmosphere is considered, important effects of entrainment of ambient air (including water vapor) are neglected. Temperature changes that may develop during the course of a day can even lead to significant changes in plume top height. Even more important seems to be the humidity at low altitudes, which in the tropics may be determined by tropical weather systems. High water vapor content of ambient air may lead to one third and more higher plumes. Therefore it is important to include environmental conditions in the computation of volcanic plume rise. Environmental conditions also determine the internal structure (concentration of ash, lapilli, water, etc.) and thus the potential of the climate impact.

Our results may be considered only qualitatively. More quantitative results are expected from a full 3-D simulation of the series of Mount Spurr (Crater Peak) eruptions in 1992, which we plan for the future. Only then we will also have a chance to directly compare our simulated results with real observations.

References

- Carey, S., and R. S. J. Sparks, Quantitative models of the fallout and dispersal of tephra from volcanic eruption columns, *Bull. Volcanol.*, **48**, 109-125, 1986.
- Chuan, R. L., Dispersal of volcano-derived particles from Mt. Erebus in the Antarctic atmosphere, *Antarctic Research Series*, **66**, 97-102, 1994.
- Dobran, F., and A. Neri, Numerical simulation of collapsing volcanic columns, *J. Geophys. Res.*, **98**, 4231-4259, 1993.
- Ernst, G. G. J., J. P. Davis, R. Stephen, and J. Sparks, Bifurcation of volcanic plumes in a crosswind, *Bull. Volcanol.*, **56**, 159-169, 1994.
- Gibson, J. K., P. Kallberg, S. Uppala, A. Nomura, A. Hernandez, and E. Serrano, 'ERA description', ECMWF re-analysis project report series, Rep. 1, Eur. Cent. for Medium-Range Weather Forecasts, Reading, England, 1997.
- Glaze, L. S., S. M. Baloga, and L. Wilson, Transport of atmospheric water vapor by volcanic eruption columns, *J. Geophys. Res.*, **102**, 6099-6108, 1997.
- Herzog, M., Simulation der Dynamik eines Multikomponentensystems am Beispiel vulkanischer Eruptionswolken, Ph.D. thesis, Max Planck Inst. for Meteorol., Hamburg, Germany, 1998.
- Herzog, M., H.-F. Graf, C. Textor, and J. M. Oberhuber, The effect of phase changes of water on the development of volcanic plumes, *J. Volcanol. Geotherm. Res.*, in press, 1999.
- Hobbs, P. V., J. P. Tuell, D. A. Hegg, L. F. Radke, and M. W. Eltgroth, Particles and gases from the 1980-1981 volcanic eruptions of Mount St. Helens, *J. Geophys. Res.*, **87**, 11,062-11,086, 1982.
- McClatchey, R. A., R. W. Fenn, J. E. A. Selby, F. E. Volz, and J. S. Garing, *Optical Properties of the Atmosphere*, 3rd ed., *Environ. Res. Pap.*, vol. 411, 1972.
- Neri, A., and G. Macedonio, Numerical simulation of collapsing volcanic columns with particles of two sizes, *J. Geophys. Res.*, **101**, 8153-8174, 1996.
- Oberhuber, J. M., M. Herzog, H.-F. Graf, and K. Schwanke, Volcanic plume simulation on large scales, *J. Volcanol. Geotherm. Res.*, in press, 1999.
- Rose, W. I., R. L. Chuan, and D. C. Woods, Small particles in the plumes of Mount St. Helens, *J. Geophys. Res.*, **87**(C), 4956-4962, 1982.
- Schmincke, H.-U., Transfer von festen, flüssigen und gasförmigen Stoffen aus Vulkanen in die Atmosphäre, *UWSF-Z. Umweltchem. Oekotox.*, **5**(1), 27-44, 1993.
- Smith, B. D., R. A. Zielinski, W. I. Rose, and B. J. Huebert, Water-soluble material on aerosols collected within volcanic eruption clouds, *J. Geophys. Res.*, **87**(C7), 4963-4972, 1982.
- Sparks, R. S. J., and L. Wilson, A model for the formation of ignimbrite by gravitational column collapse, *J. Geol. Soc. London*, **132**, 441-452, 1976.
- Textor, C., Numerical simulation of scavenging processes in explosive eruption clouds, Ph.D. thesis, Univ. of Hamburg, Hamburg, Germany, 1999.
- Valentine, G. A., and K. H. Wohletz, Numerical models of plinian columns and pyroclastic flows, *J. Geophys. Res.*, **94**, 1867-1887, 1989.
- Varekamp, J. C., E. Thomas, M. Germany, and P. R. Buseck, Particle geochemistry of volcanic plumes of Etna and Mount St. Helens, *J. Geophys. Res.*, **91**(B12), 12,233-12,248, 1986.
- Wilson, L., Explosive volcanic eruptions, III. Plinian eruption columns, *Geophys. J. R. Astron. Soc.*, **45**, 543-556, 1976.
- Wohletz, K. H., T. R. McGetchin, M. T. Sanford II, and E. M. Jones, Hydrodynamic aspects of caldera-forming eruptions: Numerical models, *J. Geophys. Res.*, **89**, 8269-8285, 1984.
- Woods, A. W., The fluid dynamics and thermodynamics of eruption columns, *Bull. Volcanol.*, **50**, 169-193, 1988.
- Woods, A. W., Moist convection and the injection of volcanic ash into the atmosphere, *J. Geophys. Res.*, **98**, 17,627-17,636, 1993.
- Woods, A. W., and M. I. Bursik, Particle fallout, thermal disequilibrium and volcanic plumes, *Bull. Volcanol.*, **53**, 559-570, 1991.
- H.-F. Graf, M. Herzog, C. Textor, Max Planck Institute for Meteorology, Bundesstr. 55, D-20146 Hamburg, Germany. (graf@dkrz.de; herzog@dkrz.de; textor@dkrz.de.)
J. M. Oberhuber, German Climate Computing Centre, Bundesstr. 55, D-20146 Hamburg, Germany.

(Received December 21, 1998; revised June 21, 1999; accepted June 29, 1999.)